

Research Article

Hybridized Extreme Learning Machine Model with Salp Swarm Algorithm: A Novel Predictive Model for Hydrological Application

Zaher Mundher Yaseen ¹, Hossam Faris,² and Nadhir Al-Ansari ³

¹*Sustainable Developments in Civil Engineering Research Group, Faculty of Civil Engineering, Ton Duc Thang University, Ho Chi Minh City, Vietnam*

²*King Abdullah II School for Information Technology, The University of Jordan, Amman, Jordan*

³*Civil, Environmental and Natural Resources Engineering, Lulea University of Technology, 97187 Lulea, Sweden*

Correspondence should be addressed to Zaher Mundher Yaseen; yaseen@tdtu.edu.vn

Received 8 August 2019; Accepted 16 January 2020; Published 21 February 2020

Guest Editor: Jesus Vega

Copyright © 2020 Zaher Mundher Yaseen et al. This is an open access article distributed under the Creative Commons Attribution License, which permits unrestricted use, distribution, and reproduction in any medium, provided the original work is properly cited.

The capability of the extreme learning machine (ELM) model in modeling stochastic, nonlinear, and complex hydrological engineering problems has been proven remarkably. The classical ELM training algorithm is based on a nontuned and random procedure that might not be efficient in convergence of excellent performance or possible entrapment in the local minima problem. This current study investigates the integration of a newly explored metaheuristic algorithm (i.e., Salp Swarm Algorithm (SSA)) with the ELM model to forecast monthly river flow. Twenty years of river flow data time series of the Tigris river at the Baghdad station, Iraq, is used as a case study. Different input combinations are applied for constructing the predictive models based on antecedent values. The results are evaluated based on several statistical measures and graphical presentations. The river flow forecast accuracy of SSA-ELM outperformed the classical ELM and other artificial intelligence (AI) models. Over the testing phase, the proposed SSA-ELM model yielded a satisfactory enhancement in the level accuracies (8.4 and 13.1 percentage of augmentation for RMSE and MAE, respectively) against the classical ELM model. In summary, the study ascertains that the SSA-ELM model is a qualified data-intelligent model for monthly river flow prediction at the Tigris river, Iraq.

1. Introduction

Due to the wide range of space and time variabilities, river flow modeling has been a critical problem in water management and hydrology [1]. The operation of many water resources system rule curves needs monthly river flow forecasts [2]. Various methods capable of forecasting river flow under different conditions with different levels of accuracy have been proposed, considerably evolving within the past decades from the simple linear equations to the complex and complicated ones. Researchers have considered various river flow forecasting methods such as the conceptual (HEC-HMS and HBV) [3–5], stochastic (AR-autoregressive and ARMA-autoregressive moving average) [6], and the physical-based (SWAT) models [7, 8].

The complex relationship between rainfall and river flow variables and the lack of sufficient hydrological data of watersheds have made data-driven models such as artificial intelligence more suitable for river flow forecasting compared to the process-based models [9]. Currently, a single method which can be employed generally for all types of basins and systems is yet to be developed. Hydrologists have currently been building reliable forecasting methods by exploiting the available and new scientific techniques such as hybrid intelligence models. The ability of hybrid AI models in addressing the associated nonlinearity and non-stationarity problems has attracted great attention in different domains [10, 11]. Likewise, this explains their wide applications in modeling the river flow in particular [12, 13] and hydrological processes in general [14].

Studies have demonstrated a wide range of forecasting accuracies using AI models with the geographic topographies of the test sites despite their success in other fields [15–18]. The development of a model that will be used to forecast in any environmental condition is an aspect yet to be explored. Researchers in water resources management engineering should be motivated by the assertion: does the integration of an optimization algorithm with AI models as hybrid intelligent models boost their predictive model accuracies? Hydrologists and intelligence system modelers, in an attempt to address the raised issue, have faced the challenge of properly selecting the input combinations known to rule the predictable accuracy of an objective predictive model for model development [19].

The literature stated a very massive implementation of the AI models for river flow modeling. These models are artificial neural network, genetic programming, fuzzy logic methods, support vector machine models, M5 tree models, complementary AI models coupled with data time series preprocessing techniques, and hybrid model [14]. Most recently, a new version of the ANN model called extreme learning machine was developed by the authors in [20], as a robust predictive model. The employment of ELM in the field of hydrology and particularly in river flow modeling demonstrated a very promising and enhancement in the modeling process [14].

The first attempt of modeling river flow using ELM was established in [21]. The authors developed an ELM model to capture the associated nonlinearity of the seasonal river inflow of the Brazilian Hydropower. Their Finding evidenced the potential of the proposed model and emphasised several hydrological investigations later on. Li and Cheng [22] studied the capacity of ELM to modulate the monthly scale reservoir inflow in China. The ELM model provided an accurate result in comparison with several other well-established AI models. An improved ELM model is developed in a new version called online sequential extreme learning machine (OS-ELM) for multiple river flow scales prediction in Canada [22]. The same OS-ELM model was developed for flood events forecasting for hourly river flow monitoring [23]. The findings of the improved ELM model demonstrated a noticeable prediction performance. In another attempt, Yaseen et al. developed an ELM model to forecast the monthly scale river flow located in semiarid environment in Iraq. The proposed model revealed good capability to mimic the monthly river flow trend. Later on, several studies approved the potential of the ELM in the field of hydrology processes [13, 24–29]. Based on the reported literature of the extreme learning machine modeling and its version improvement in hydrological problems over a very short period, the authors' attention is mainly to modify this robust predictive model and attempt to enhance its predictability skills.

Despite the noticeable promising implementation of the ELM model in wide range of hydrology applications, it still suffers limitations and drawbacks. First, the random assignment of the input weights and biases can negatively affect the generalization capability of the network [30]. In addition, ELM needs larger number of hidden neurons

which results in more complex models [31]. Hence, the main motivation of the current research is to propose a new training optimization for the ELM model to solve the aforementioned problems and improve the predictability performance of the ELM model.

In this research, a new optimization algorithm called Salp Swarm Algorithm is proposed and hybridized with the ELM model for optimizing the input weights and hidden biases of the network. SSA is a modern nature-inspired algorithm proposed in [32]. SSA has shown an impressive performance in optimizing various complex and challenging engineering problems. Based on these facts, the motivation of exploring the capabilities of this optimizer is endeavoured and the authors work to improve the performance of the classical ELM model for the surface hydrology application. For this reason, a real case of semiarid environment of the Tigris river in Iraq is investigated which is an extension for the published work [33].

This research is organized as following. A brief introductory of the proposed methodology is given in Section 2. The description of the investigated case study is described in Section 3. The proposed ELM model based on the SSA optimizers is introduced and discussed in detail in Section 4. The experiments and results are given and discussed in Section 5. Finally, the conclusions and findings of this work are summarized in Section 6.

2. Preliminaries

2.1. Salp Swarm Algorithm. SSA is a recent nature-inspired algorithm which mimics the swarming behaviour of sea creatures called salps [32]. Salps have barrel-shaped gelatinous bodies, and they move around by pumping water through their body from one side to the other. Salps exist as colonies and move together as chains. In SSA, the movement behaviour is mathematically modelled for solving optimization problems. The models suppose that there are two main types of salps: leaders and followers. The leaders are the salps that lead the chain in the front direction, while the followers follow their leaders synchronously and in harmony as shown in Figure 1.

Like all swarm intelligent algorithms, SSA starts by randomly initializing a swarm of N salps. Each salp is represented by one-dimensional vector of n elements, while the swarm is represented as a two-dimensional matrix x . The algorithm also refers to the target of the swarm as a food source F . The movement of the leader chain x_j^1 is modelled as given in the following formula:

$$x_j^1 = \begin{cases} F_j + c_1((ub_j - lb_j)c_2 + lb_j), & c_3 \geq 0.5, \\ F_j + c_1((ub_j - lb_j)c_2 + lb_j), & c_3 < 0.5, \end{cases} \quad (1)$$

where j is the dimension of the position to be updated, F_j is the j th element of the food source position, ub_j and lb_j are the upper and lower bounds of the j th element, c_2 and c_3 are the random numbers drawn from the interval $[0, 1]$, and c_1 is the dynamic variable that changes its value over the course of iterations according to the following formula:

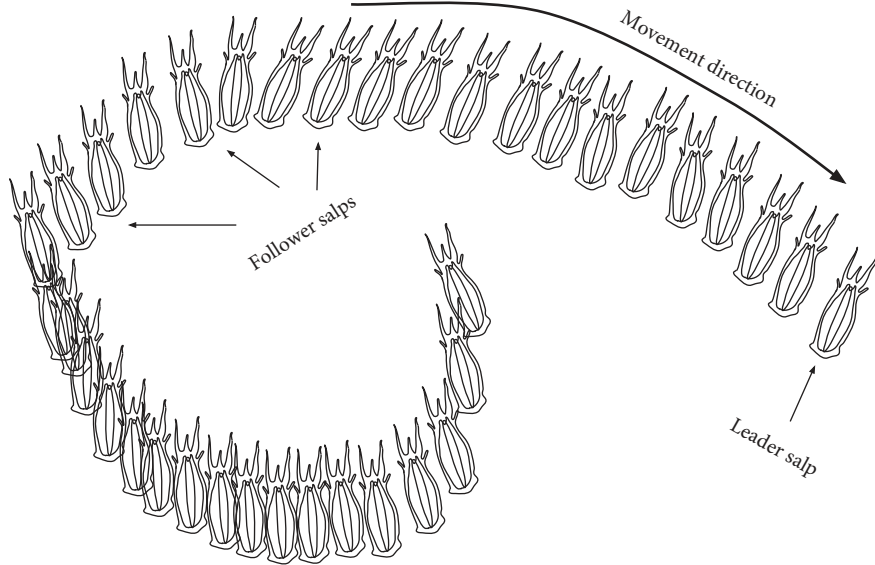


FIGURE 1: Leaders and followers of salps chain movement.

$$c_1 = 2e^{-(4l/L)^2}, \quad (2)$$

in which l represents the current iteration and L is a predefined number of maximum iterations. Note that c_1 is a very important variable in the SSA process which controls the balance between the exploration and exploitation processes of the optimization algorithm. The followers update their position accordingly as

$$x_j^i = 0.5(x_j^i - x_j^{i-1}), \quad (3)$$

where x_j^i is the i th element of the j th position and $i \geq 2$. The procedure of the SSA algorithm is presented in Figure 2.

2.2. Extreme Learning Machines. Artificial neural networks (ANN) have been used as a universal approximator to deal with complex problems in a wide spectrum of different domains. One of these common problems is classification and regression problems. For ANN to be able to predict the value of the output variable, it needs to be trained based on a set of examples using a learning algorithm. One of the recent and successful variants of ANNs is ELM. ELM is a learning framework for single hidden layer feedforward neural networks (SLFN) introduced recently in [20]. The main merit of the ELM model is the learning process convergence speed that emphasizes the capability over the classical gradient decent approach for training the SLFN [34]. In addition, the nonrequirement for algorithm tuning parameters is similar to the back-propagation algorithm. The ELM model requires no human interactive for tuning [35]. Further, ELM does not require an iterative process to tune the SLFN parameters. Instead, it randomly modifies the input weights and the hidden biases and then it governs the output weights systematically using the potential of the Moore–Penrose (MP) generalized inverse method. An illustration of the SLFN-based ELM is shown in Figure 3.

Pseudocode of the SSA algorithm.

```

Initialize a swarm of slaps  $x_i (i = 1, 2, \dots, n)$ 
While (Termination condition is not met) do
  Calculate the fitness of each salp in the swarm
  Set F as the position of best salp
  Update  $c_1$  by equation (2)
  for (each salp ( $x_i$ )) do
    if ( $i == 1$ ) then
      Update the leader's position using equation (1)
    else
      Update the follower's position using equation (3)
    end if
  end for
  Check and return salps if they go beyond upper and
  lower bounds
end while
Return F

```

FIGURE 2: Salp Swarm Algorithm procedure.

The output of SLFN is trained using a dataset with N distinct examples denoted as $(x_i, t_i), i = 1, 2, \dots, N$, where x_i is the input vector and t_i is the output vector. The activation function $g(\cdot)$ and k hidden neurons is

$$f_i = \sum_{j=1}^k \beta_j g(w_j x_i + b_j), \quad j = 1, 2, \dots, N, \quad (4)$$

where w_j denotes the weight vector that links the input nodes to the j th hidden node, b_j signifies the bias value of the j th hidden node, and β_j are the values of the output weights that connect the j th hidden node with the output nodes [36]. Formula (4) is written compactly as

$$O = H \times \beta, \quad (5)$$

where H is the output matrix of the hidden layer. ELM assigns the weights and the biases randomly without the need to take into consideration the input data. ELM determines the output weights by solving equation (5) using

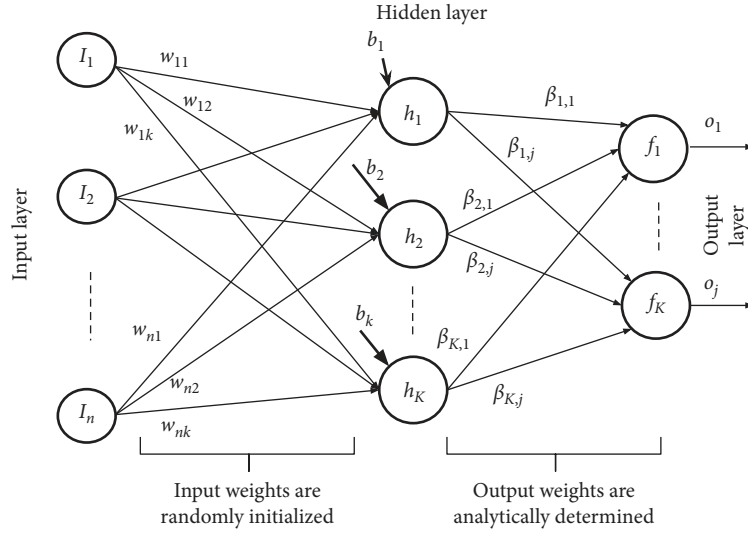


FIGURE 3: The architecture of the single hidden layer ELM model.

MP generalized inverse. The output weights can be determined by ELM using the following formula:

$$\hat{\beta} = H^\dagger \times T. \quad (6)$$

The process of the ELM predictive model is presented in Figure 4.

3. Case Study and Site Description

In this study, the Tigris river which is located in the Iraq region is selected for examining the proposed hybrid predictive model. The total length of the river is around 1718 km. The river originates from Turkey and flows toward Iraq in the southern part. Most of the river basin (about 85 percentage) is located in Iraq with an approximate catchment area of 253000 km². Tigris and Euphrates rivers are presenting the chief freshwater resources in Iraq, providing water for multiple usages such as domestic, agricultural, industrial uses, and several other usages. The region environment of the river has a semiarid climate, with the Tigris basin having a climatic range from semihumid in the headwaters to the north to semiarid in the area close to where it met with the Euphrates river in the southern part of the region. The average precipitation in the basin per year is between 400 and 600 mm, even though the annual precipitation values in the upper and lower parts have been registered as 800 and 150 mm, respectively. Due to the high precipitation rates in the Zagros Mountains in the east of the Tigris basin, it has a significantly higher mean precipitation of approximately 300 mm/year compared to the Euphrates basin [37]. Precipitation mainly occurs in the basins around November and April, while January to March witness snowfall in the mountains. The climatic conditions in the lowlands of Iraq and Syria (semiarid to arid) usually facilitate a considerable loss of water to evapotranspiration in the Mesopotamian region. The Tigris basin has an air temperature of about -35°C during the winter in the Armenian Highlands and about 40°C on the Jezira plateau during the

ELM algorithm for training SLFN.

Input: $L = \{(x_i, t_i) \mid x_i \in R^m, t_i \in R^m, i = 1, 2, \dots, N\}$

// Training dataset L consists of a set of N training samples and their associated output values.

$g(x)$: activation function.

\tilde{N} : Number of hidden nodes

Output: Output weight $\hat{\beta}$

(1) procedure ELM($L, N, g(\cdot)$)

(2) Initialize weights w_i and biases b_i randomly $[-1, 1]$, $i = 1, 2, \dots, \tilde{N}$.
 $\triangleright w_i$ is the vector of weights that connect the hidden node i to all input nodes.
 $\triangleright b_i$ is the bias value of the hidden node i

(3) Calculate the hidden layer output matrix H

$$H = \begin{bmatrix} g(w_1 \cdot x_1 + b_1) & \dots & g(w_{\tilde{N}} \cdot x_1 + b_{\tilde{N}}) \\ \vdots & & \vdots \\ g(w_1 \cdot x_N + b_1) & \dots & g(w_{\tilde{N}} \cdot x_N + b_{\tilde{N}}) \end{bmatrix}$$

(4) Find output weight $\hat{\beta}$ using MP generalized inverse

$$\hat{\beta} = H^\dagger T$$

$$\hat{\beta} = (H^T H)^{-1} H^T T$$

(5) return $\hat{\beta}$

\triangleright The output weights

(6) end procedure

FIGURE 4: The extreme learning machine model learning procedure.

summer [38]. Baghdad, the capital city of Iraq, has an average rainfall of about 216 mm, with rainfall usually experienced from December to February. At the capital, the Tigris river mean river flow is 235 m³·s⁻¹. The maximum weather temperature experienced around is 45°C during the summer and about 10°C during the winters [39, 40].

For the modeling establishment, the monthly river flow scale is used to build the predictive model measured at the Baghdad station (see Figure 5). The historical river flow database is gathered from the USGS Data Series 540 [41]. The statistical description of the utilized dataset is tabulated in Table 1. The area of the drainage site is 134, 000 km², which is



FIGURE 5: The case study location: Baghdad metrological station, Tigris river, Iraq.

TABLE 1: Descriptive statistics for the mean monthly river flow for the Tigris river at Baghdad (Iraq) (1991–2010) [33].

Partition	Time period	No. records	Q ($\text{m}^3 \cdot \text{s}^{-1}$)				
			Mean	St. dev.	Median	Minimum	Maximum
Training	Jun. 1991–Dec. 2007	187	780.099	379.712	674.700	298.100	2651.000
Testing	Jan. 2007–Dec. 2010	48	489.879	136.746	445.900	331.400	936.400
Complete	Jun. 1991–Dec. 2010	235	720.820	363.469	636.900	298.100	2651.000

coordinated between the Latitude of $33^\circ 24' 34''\text{N}$ and a Longitude of $44^\circ 20' 32''\text{E}$. Over the past two decades, a noticeable negative river flow deterioration was observed for the Tigris river. This deterioration is associated with several causes such as diplomatic issues or climate change. Hence, the necessity of providing an accurate and reliable data-intelligence model for this river system is highly recommended.

4. Proposed SSA-ELM Forecasting Model

There are two basic points that should be determined before applying any evolutionary or swarm-based algorithm to optimize any problem which are the representations of the solution and the choice of the cost function. These two points are addressed for the proposed SSA-ELM model as follows:

- (i) In order to handle an optimization problem using a metaheuristic algorithm, the solution of the problem should be represented properly in the algorithm. That is, the way that the solution is encoded as an individual. In the proposed SSA-ELM model, each individual represents a potential solution as a real

vector I , where I consists of two parts: inputs weights and hidden biases as given in equation (10). All elements of I are generated in $[-1, 1]$:

$$I = [W_{11}, W_{12}, \dots, W_{nk}, b_1, \dots, b_k]. \quad (7)$$

- (ii) In all metaheuristic algorithms, a cost function is utilized to assess the quality of the generated solutions over the course of iterations. In this work, the root mean squared error (RMSE) is selected as the cost function which is the most commonly used cost function in evolutionary extreme learning algorithms. RMSE can be measured as given in equation (8). The goal of the algorithm is to find the ELM model that has the minimum value of RMSE:

$$\text{RMSE} = \sqrt{\frac{\sum_{j=1}^N \left\| \sum_{j=1}^K \beta_j g(w_j x_i + b_j) - t_i \right\|^2}{m \times N}}. \quad (8)$$

The procedure of the proposed SSA-ELM algorithms can be described as follows:

First, the algorithm starts by generating randomly a predefined number N of particles. Each of the particles represents a candidate ELM network as explained previously.

Then, the fitness of each particle is calculated using the following steps:

- (i) Assign the values of the input weights and hidden biases that a given particle carries to a network structure.
- (ii) Calculate the output weights of the ELM network using the PM method based on the training part of the dataset.
- (iii) Calculate the RMSE as given in equation (8) based on the validation part of the dataset.

After performing the fitness evaluation step, the particles are sorted according to their fitness values. The best L particles that generate ELM networks with lowest RMSE values are nominated as leaders. The rest of the particles in the swarm are considered as followers. The description of the proposed predictive algorithm is displayed in Figure 6.

The positions of the leaders and followers are updated according to equations ((1) and (3)), respectively. The evaluation and update steps are repeated until a predefined number of iterations is reached.

The training procedure of the proposed model is established using correlated lags computed via the correlations statistical approach (i.e., autocorrelation and partial autocorrelation functions) to detect appropriate input attributes to the targeted attribute (see Figure 7). This process is accomplished in harmony with major researches of the literature [42, 43]. Based on the visualization of the correlation statistic, five lags time of river flow historical information (attributes variables) influence the one-step ahead river flow modeling. Hence, a combination of five scenarios model (M1, M2, . . . , M5) architecture is constructed as follows:

$$\begin{aligned}
 \text{Model 1} \quad & \text{M1: } Q_{(t)} = fQ_{(t-1)}, \\
 \text{Model 2} \quad & \text{M1: } Q_{(t)} = fQ_{(t-1)}, Q_{(t-2)}, \\
 \text{Model 3} \quad & \text{M1: } Q_{(t)} = fQ_{(t-1)}, Q_{(t-2)}, Q_{(t-3)}, \\
 \text{Model 4} \quad & \text{M1: } Q_{(t)} = fQ_{(t-1)}, Q_{(t-2)}, Q_{(t-3)}, Q_{(t-4)}, \\
 \text{Model 5} \quad & \text{M1: } Q_{(t)} = fQ_{(t-1)}, Q_{(t-2)}, Q_{(t-3)}, Q_{(t-4)}, Q_{(t-5)},
 \end{aligned} \tag{9}$$

where $Q_{(t)}$ is the target river flow step ‘‘one month ahead’’ and $Q_{(t-1)}, \dots, Q_{(t-5)}$ are the lag times up to five months previously. Here, five input combinations are constructed for the prediction matrix of the SSA-ELM and ELM predictive models.

5. Application Results and Analysis

Over the past couple decades, massive attention has been focused on hydrological time series modeling, particularly for river flow process. This is owing to the need of an accurate and reliable intelligent model that can be implemented in real practice. Several machine learning approaches have been proposed to forecast and simulate the river flow time series. As a matter of fact, the assumption of

the hydrological time series is originated by stochasticity, nonlinearity, and redundancy. Also, the underlying mechanisms of river flow generation are mostly different from low-, medium-, and high-flow periods. In other words, the extreme events of flows rely upon the outburst of heavy storm of rainfall events. Hence, developing a new data-intelligent model characterized by sophistication to forecast all kind of flow patterns satisfactory is still under process mission for the hydrology engineers. In this research, the application of forecasting the monthly river flow (semiarid environment) using the hybrid SSA-ELM model is presented. Indeed, using a univariate modeling is more challenging for the hydrologist as it is fulfilled for the benefit of the catchment that lacks the metrological information.

The perdition skills for the conducted modeling were carried out using two types of performance indicators including the goodness (e.g., (r) and (WI)) and the absolute error measures (e.g., (RMSE) and (MAE)). The mathematical description of these performance indicators is

$$r = \frac{\sum_{i=1}^{i=N} [(S_i^{\text{obs}} - \overline{S^{\text{obs}}}) \cdot (S_i^{\text{pred}} - \overline{S^{\text{pred}}})]}{\sqrt{\sum_{i=1}^{i=N} (S_i^{\text{obs}} - \overline{S^{\text{obs}}})^2} \cdot \sqrt{\sum_{i=1}^{i=N} (S_i^{\text{pred}} - \overline{S^{\text{pred}}})^2}}$$

where $-1 \leq r \leq 1$

$$\text{WI} = 1 - \left[\frac{\sum_{i=1}^{i=N} (S_i^{\text{obs}} - S_i^{\text{pred}})^2}{\sum_{i=1}^{i=N} (|S_i^{\text{pred}} - \overline{S^{\text{obs}}}| + |S_i^{\text{obs}} - \overline{S^{\text{obs}}}|)^2} \right], \tag{10}$$

$$\text{RMSE} = \sqrt{\frac{1}{N} \sum_{i=1}^{i=N} (S_i^{\text{obs}} - S_i^{\text{pred}})^2},$$

$$\text{MAE} = \frac{1}{N} \sum_{i=1}^{i=N} |S_i^{\text{obs}} - S_i^{\text{pred}}|,$$

where S_i^{obs} and S_i^{pred} are the observed and forecasted values of river flow, $\overline{S^{\text{obs}}}$ and $\overline{S^{\text{pred}}}$ are the mean values of river flow, and N is the number of the observations of the testing phase.

For SSA, the size of the population is set to 50 while the number of iterations is set to 1000. These values were recommended and showed superior results when applied for solving complex optimization problems in [32]. For ELM, the common sigmoid function activation function is used [44]. However, the number of hidden nodes was systematically determined by experimenting different numbers starting from 2 hidden nodes up to 10 with a step of 2 nodes each time.

Table 2 tabulates the efficiency results of the hybrid SSA-ELM model achieved based on the testing data for each input combination attribute. The results are validated against the published results of ELM, support vector regression (SVR), and generalized regression neural network (GRNN) which were conducted in [33], on the same case study. In addition, Table 2 also lists the results of random forests (RF) implemented in Weka the popular suite of machine learning software [45].

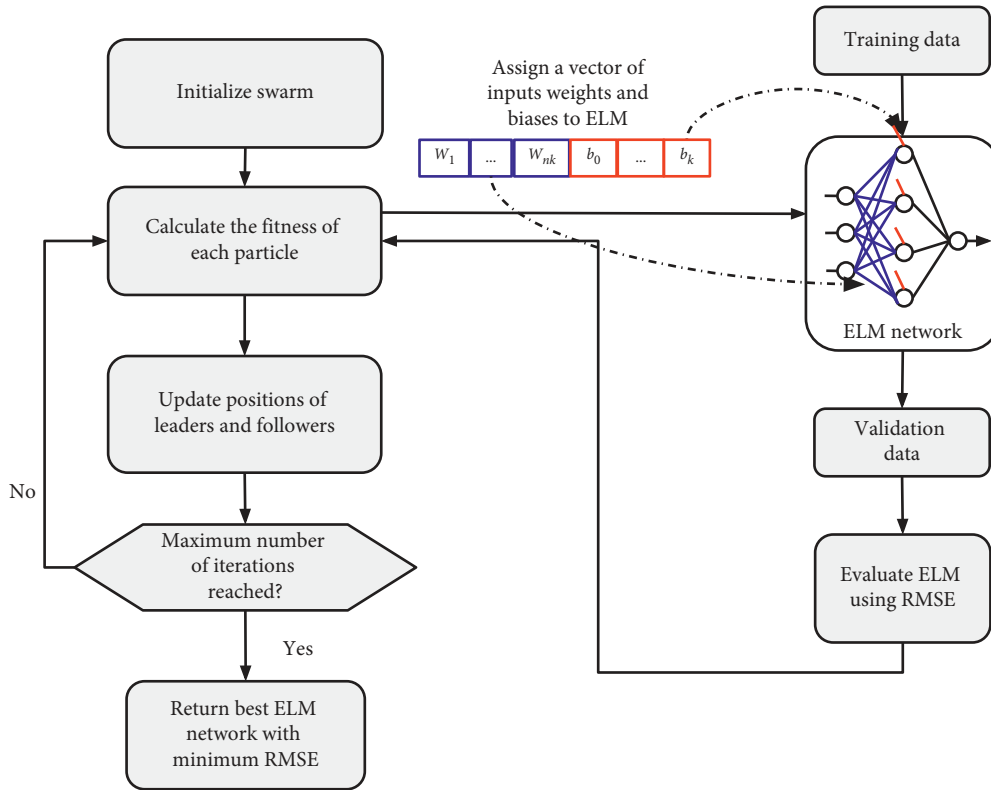


FIGURE 6: Description of the proposed SSA-ELM algorithm.

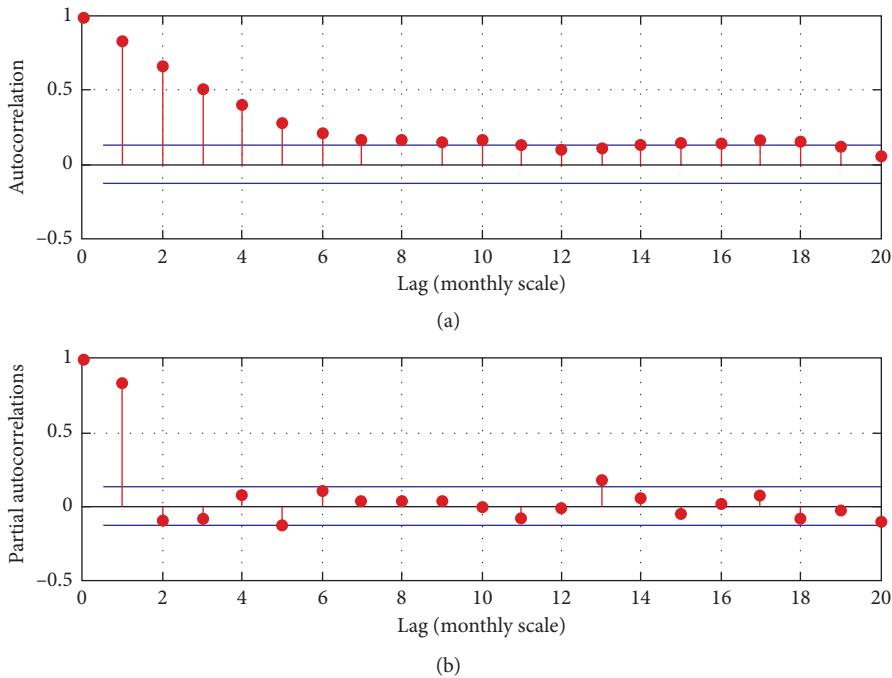


FIGURE 7: The statistical correlation process function of the investigated monthly scale river flow.

Indeed, the motivation of the current study is to improve the performance of the nontuned predictive model ELM through complementing with an evolutionary nature-inspired novel optimization algorithm (i.e., SSA). Based on the

investigated results, an excellent performance in terms of lower RMSE and MAE values and higher r and WI values, respectively, when forecasting the present river flow data, was observed. The results exhibited a noticeable

TABLE 2: Performance evaluation for ELM and SSA-ELM, SVR, GRNN, and RF models.

Input combinations	Models	r	WI	RMSE ($\text{m}^3 \cdot \text{s}^{-1}$)	MAE ($\text{m}^3 \cdot \text{s}^{-1}$)
M1	SSA-ELM	0.812	0.861	80.592	66.203
	ELM	0.81	0.82	98.272	87.012
	SVR	0.761	0.802	106.749	90.905
	GRNN	0.658	0.689	127.818	113.698
	RF	0.372	0.531	189.778	131.966
M2	SSA-ELM	0.809	0.850	80.516	62.185
	ELM	0.817	0.834	95.571	83.899
	SVR	0.715	0.769	111.228	95.14
	GRNN	0.468	0.54	125.187	103.551
	RF	0.373	0.549	175.765	142.347
M3	SSA-ELM	0.784	0.812	86.868	62.185
	ELM	0.815	0.814	104.307	92.544
	SVR	0.741	0.776	118.02	101.85
	GRNN	0.496	0.54	125.187	103.551
	RF	0.037	0.33	280.85	225.27
M4	SSA-ELM	0.800	0.855	87.84	69.069
	ELM	0.803	0.826	98.432	85.117
	SVR	0.728	0.769	119.539	106.585
	GRNN	0.346	0.507	133.522	114.063
	RF	0.127	0.39	1246.48	196.745
M5	SSA-ELM	0.801	0.856	87.659	67.886
	ELM	0.799	0.853	87.906	71.544
	SVR	0.715	0.768	124.155	108.367
	GRNN	0.248	0.416	135.35	112.606
	RF	0.222	0.0001	668.76	657.031

enhancement in the prediction skills using the proposed SSA-ELM model in comparison with the benchmark ELM-based model. The improved performance with SSA-ELM attributed to the robustness of the novel evolutionary optimization method SSA linked to the ELM model. This robustness may have contributed to the internal function parameter optimization for each input combination.

The Taylor diagram is another modern graphical presentation to diagnose the predictability of the modeling through visualizing the errors from the benchmark observed record. This diagram graphically summarizes the model's efficiency in approximating the accuracy to the observed data. The Taylor diagram of the hybrid SSA-ELM and classical ELM is illustrated in Figure 8. The position of each model appeared on the diagram measures the accuracy of that model in accordance to the observed river flow. Based on the diagram presentation, the SSA-ELM model has a higher value of correlation compared to the ELM model. The SSA-ELM model approximated well with observed and located nearer to the actual record. The RMSE between the predicted and observed river flow was denoted as proportional to the distance to the point of the observation. The standard deviation of the predictive model is proportional to the radial distance from the origin.

For detailed inspection for the performance of the SSA-ELM model over the benchmark ELM model, Figure 9 presents the relative error (RE) distribution indicator in the form of boxplot. Based on the generated graph, the hybrid SSA-ELM performed an acceptable improvement with average RE between -10 and $+10\%$ and over 80% of the testing period. The maximum RE magnitude recorded on the

overestimation is $+35\%$, whereas the underestimation aspect is recorded as -25% . This is much different from the classical ELM that exceeded the -40% in the underestimation aspect.

Scatter plots for the ELM and SSA-ELM models are presented in Figures 10 and 11, respectively. The graphical presentation followed the determination coefficient values as it is the square value. The proposed hybrid model was performed closer to the ideal line between the observed and forecasted values.

It is an excellent fashion of evaluating the current research results by comparing with modern established researches with the regards of hybrid evolutionary nature-inspired algorithms integrated with AI-predictive models. Most recently, the applications of metaheuristic techniques have shown an extensive and noticeable optimization methods for AI predictive models. This is owing to the main advantages such as flexibility, give an optimal solution, and free from gradient decent drawbacks [32]. In the last five years, there are various successful attempts on hybridizing the AI models with evolutionary optimization algorithms in the field of hydrology. For instance, a combination between the adaptive neurofuzzy system (ANFIS) model with the firefly algorithm (FFA) was conducted for modeling the roller length of the hydraulic jump [46]. An integration of the classical multilayer perceptron with FFA for pan evaporation process is given in [47]. River flow forecasting for tropical environment was established using the ANFIS-FFA model [48]. On the same region of the case study implemented in this research, the water quality index prediction model was developed based on the hybridization of the support vector machine model

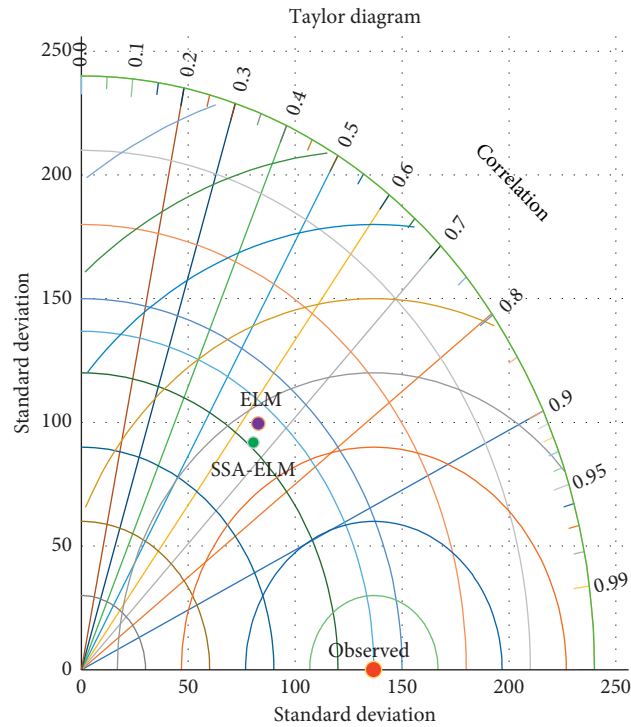


FIGURE 8: Taylor diagram graphical presentation for the ELM and SSA-ELM predictive models.

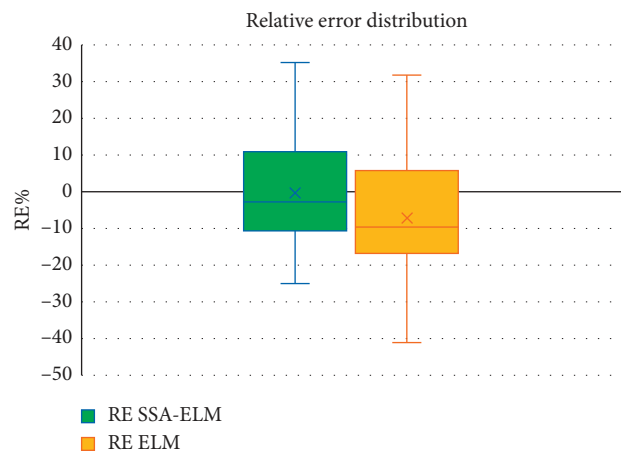


FIGURE 9: Relative error distribution percentage of SSA-ELM and ELM models.

with the firefly algorithm [49]. All the examples exhibited earlier on the hybrid models demonstrated an excellent performance over the AI-based models. It is evidenced that the present study was performed in harmony with a new era of the hybrid intelligent models in the field of surface hydrology.

For the best knowledge of the practical implementation, the proposed hybrid intelligence SSA-ELM model has the possibility of the online learning potential. As reported in Figure 12, the scheme demonstrated the capacity of the online forecasting system in which there is a possibility to be practiced as a flooding warning system. The online forecasting system starts by obtaining the metrological information (e.g.,

river flow velocity (V), cross section area (A), and river discharge (Q)) using sensors device. The data information was transferred via cricket wireless and digitized into a comma separated value (CSV) format in which it is readable by any software environment. At this stage, the learning process based on the historical records is conducted using the SSA-ELM predictive model. The outcome of the predictive model was subjected to a specific range of river flow threshold values. If the prediction value is within the threshold, the loop of the learning process is repeated using the new recalled historical information. Otherwise, if the prediction is out of the threshold range, a notification of the alarm system is integrated (global system for mobile communications) that can

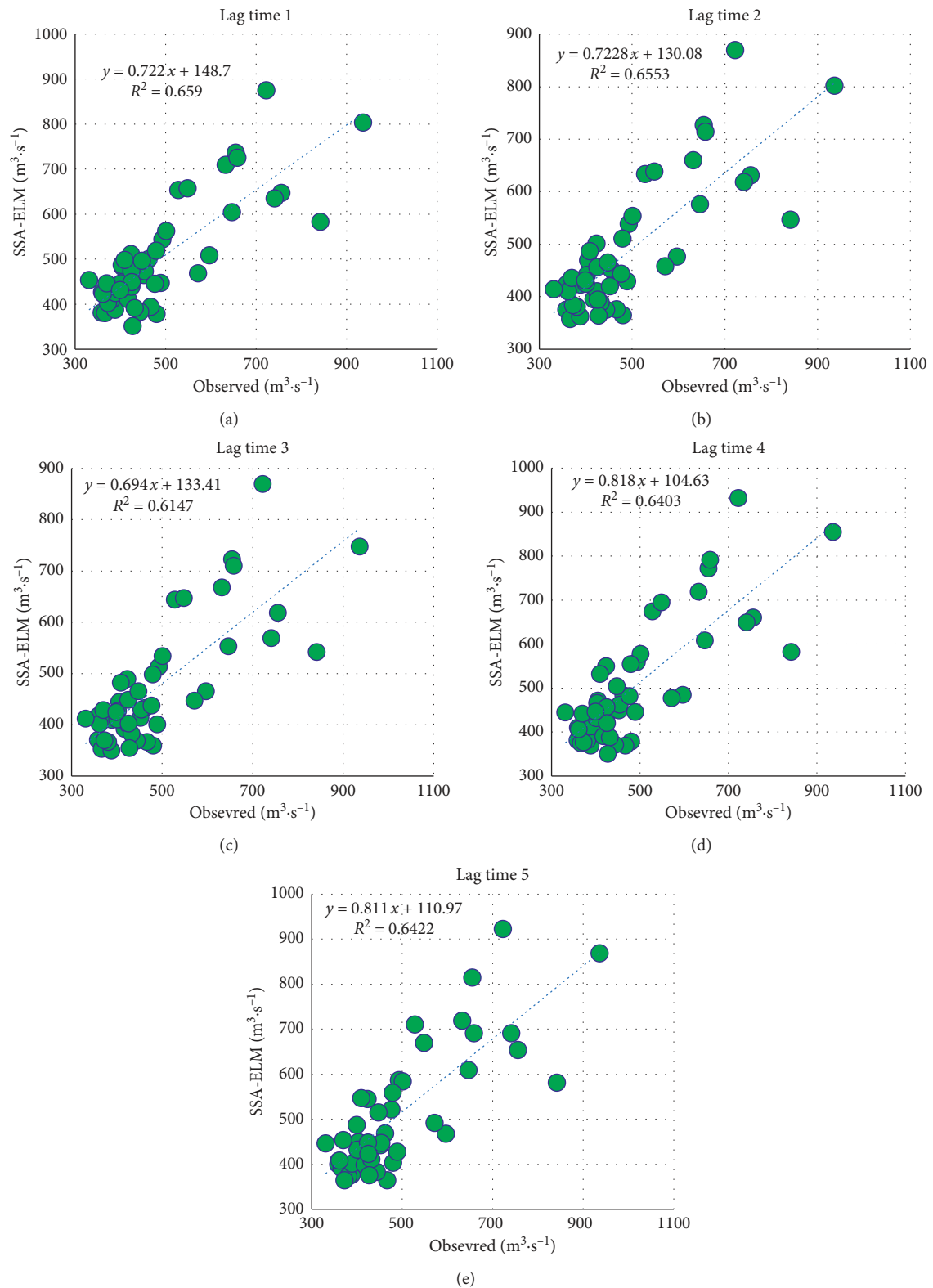


FIGURE 10: Scatter plot variation between the observed and forecasted river flow using the SSA-ELM model and for the five input combinations.

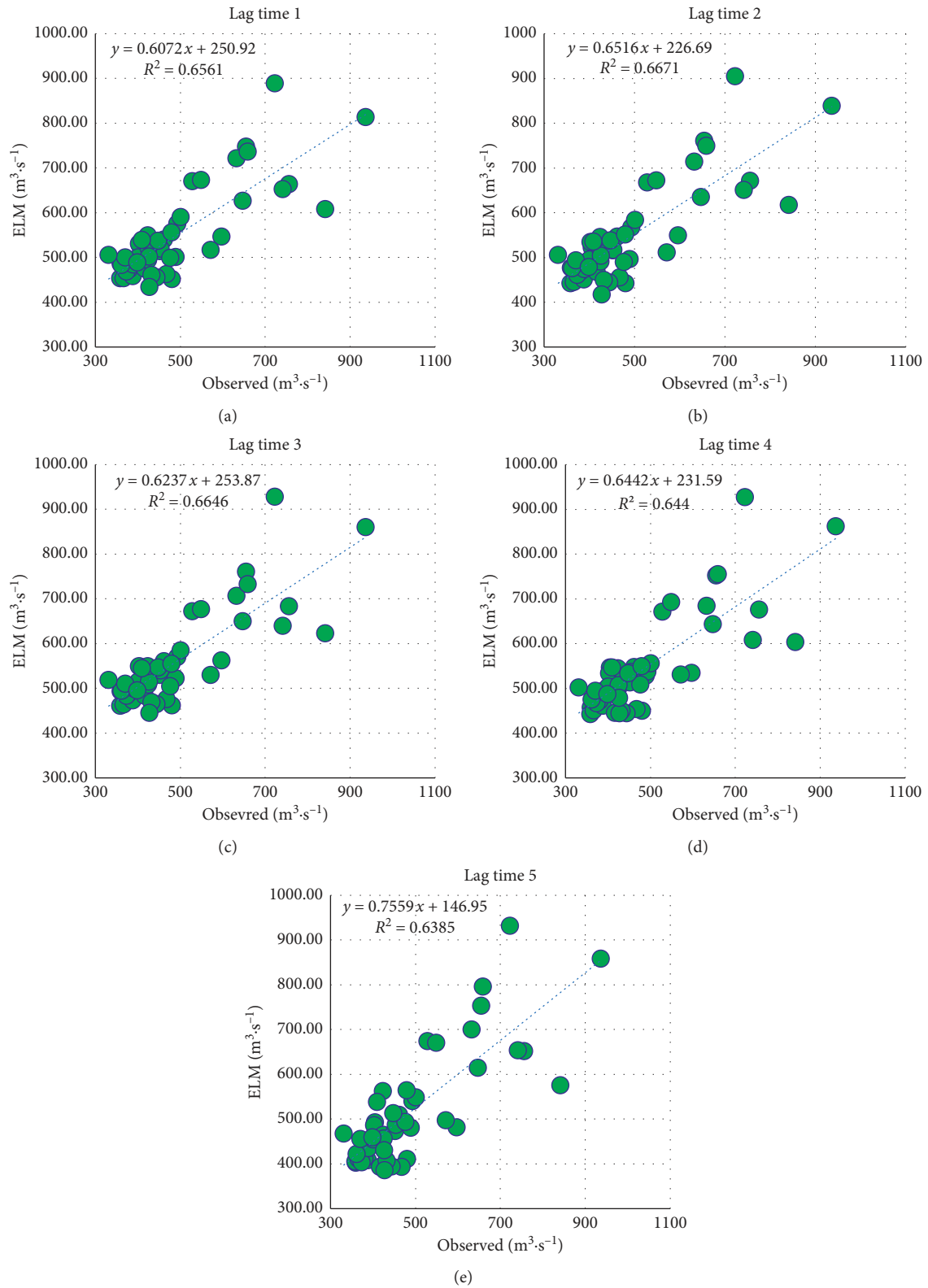


FIGURE 11: Scatter plot variation between the observed and forecasted river flow using the ELM model and for the five input combinations.

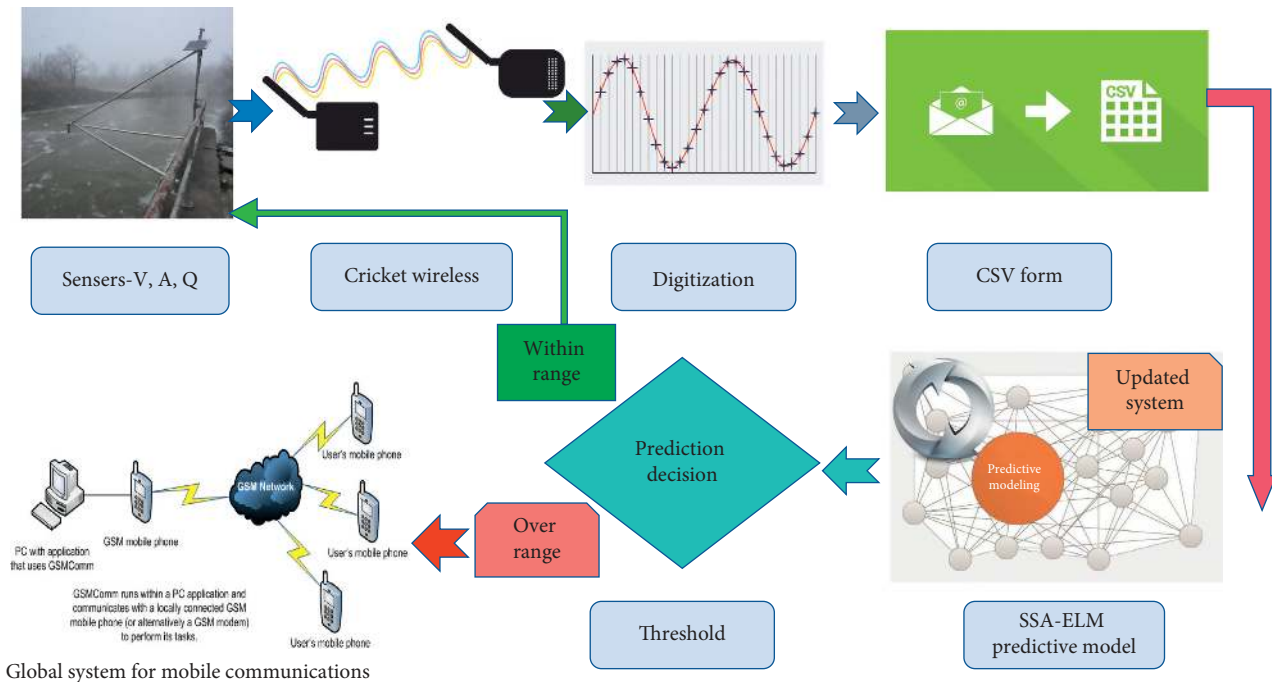


FIGURE 12: A proposition for online forecasting system based on the proposed methodology.

deliver a message of alarm to the nearby civilian for preparing an emergency evacuation. This merit can contribute remarkably to the water resources engineering, river management, and monitoring perspective.

6. Conclusions

In this research, a novel hybrid intelligent predictive model was developed to be implemented on a regression hydrological problem (i.e., river flow forecasting). A new nature-inspired optimization algorithm called Salp Swarm Algorithm was integrated with the modern AI model (i.e., ELM model) to build a robust intelligent predictive model. The basic concept of the introduced SSA is inspired from the swarming behaviour of the salp chain. The developed SSA-ELM model was applied for monthly time scale river flow data located in semiarid environment in the Iraq region. Twenty years over the period (1991–2010) was used to design the training and testing phases following the published research [33]. Several input combination attributes were investigated in accordance with the most correlated lag times. The hybrid SSA-ELM model exhibited an excellent level of accuracies in comparison with the ELM-based model. In numerical evaluation, the SSA-ELM model demonstrated an acceptable level of augmentation with regards to the absolute metrics (8.4 and 13.1% for RMSE and MAE, respectively). On the other aspect, the results verified that the lag time as an input attribute is very significant on the modeling performance of the predictive model. In conclusion, the developed model outcomes enthruse for proposing an online forecasting system that can be applied as a real-time monitoring river engineering practice. For future work, further research can be conducted based on investigating the efficiency of the proposed model by incorporating several hydrological

processes such as rainfall, humidity, wind speed, and others in modeling the target output river flow [50]. In addition, inspecting longer data span of historical data information is highly recommended to be devoted as it is a limitation of the current research. On the algorithmic level, the proposed model can be extended in a way that other parameters in the ELM network can be optimized and such parameters include the number of hidden nodes in the hidden layer, the transfer functions, and the activation functions [51–53].

Data Availability

The data used to support the findings of this study are available from the corresponding author upon request.

Conflicts of Interest

The authors have no conflicts of interest to declare.

References

- [1] J. Patskoski and A. Sankarasubramanian, "Reducing uncertainty in stochastic streamflow generation and reservoir sizing by combining observed, reconstructed and projected streamflow," *Stochastic Environmental Research and Risk Assessment*, vol. 32, no. 4, pp. 1065–1083, 2018.
- [2] F. Fathian, A. Fakheri-Fard, T. Ouarda, Y. Dinpashoh, and S. S. M. Nadoushani, "Multiple streamflow time series modeling using VAR-MGARCH approach," *Stochastic Environmental Research and Risk Assessment*, vol. 32, no. 2, pp. 407–425, 2019.
- [3] M. Azmat, M. Choi, T.-W. Kim, and U. W. Liaqat, "Hydrological modeling to simulate streamflow under changing climate in a scarcely gauged cryosphere catchment," *Environmental Earth Sciences*, vol. 75, no. 3, pp. 1–16, 2016.

- [4] K. Stahl, R. D. Moore, J. M. Shea, D. Hutchinson, and A. J. Cannon, "Coupled modelling of glacier and streamflow response to future climate scenarios," *Water Resources Research*, vol. 44, 2008.
- [5] A. K. Verma, M. K. Jha, and R. K. Mahana, "Evaluation of HEC-HMS and WEPP for simulating watershed runoff using remote sensing and geographical information system," *Paddy and Water Environment*, vol. 8, no. 2, pp. 131–144, 2010.
- [6] R. Modarres and S. S. Eslamian, "Streamflow time series modeling of Zayandehrud River," *Iranian Journal of Science and Technology, Transaction B: Engineering*, vol. 30, pp. 567–570, 2006.
- [7] I. Masih, S. Maskey, S. Uhlenbrook, and V. Smakhtin, "Assessing the impact of areal precipitation input on streamflow simulations using the SWAT Model1," *JAWRA Journal of the American Water Resources Association*, vol. 47, no. 1, pp. 179–195, 2011.
- [8] K. Rahman, C. Maringanti, M. Beniston, F. Widmer, K. Abbaspour, and A. Lehmann, "Streamflow modeling in a highly managed mountainous glacier watershed using SWAT: the upper Rhone River watershed case in Switzerland," *Water Resources Management*, vol. 27, no. 2, pp. 323–339, 2013.
- [9] Z. M. Yaseen, A. El-shafie, O. Jaafar, H. A. Afan, and K. N. Sayl, "Artificial intelligence based models for streamflow forecasting: 2000–2015," *Journal of Hydrology*, vol. 530, pp. 829–844, 2015.
- [10] W. Hu, L. Yan, K. Liu, and H. Wang, "A short-term traffic flow forecasting method based on the hybrid PSO-SVR," *Neural Processing Letters*, vol. 43, no. 1, pp. 155–172, 2016.
- [11] Z. M. Yaseen, O. Kisi, and V. Demir, "Enhancing long-term streamflow forecasting and predicting using periodicity data component: application of artificial intelligence," *Water Resources Management*, vol. 30, no. 12, pp. 4125–4151, 2016.
- [12] A. Danandeh Mehr, E. Kahya, F. Bagheri, and E. Deliktas, "Successive-station monthly streamflow prediction using neuro-wavelet technique," *Earth Science Informatics*, vol. 7, no. 4, pp. 217–229, 2013.
- [13] R. C. Deo and M. Şahin, "An extreme learning machine model for the simulation of monthly mean streamflow water level in eastern Queensland," *Environmental Monitoring and Assessment*, vol. 188, no. 2, 2016.
- [14] Z. M. Yaseen, S. O. Sulaiman, R. C. Deo, and K.-W. Chau, "An enhanced extreme learning machine model for river flow forecasting: state-of-the-art, practical applications in water resource engineering area and future research direction," *Journal of Hydrology*, vol. 569, pp. 387–408, 2019.
- [15] H. Jiang and Y. Dong, "A novel model based on square root elastic net and artificial neural network for forecasting global solar radiation," *Complexity*, vol. 2018, Article ID 8135193, 19 pages, 2018.
- [16] B. B. Sahoo, R. Jha, A. Singh, and D. Kumar, "Application of support vector regression for modeling low flow time series," *KSCE Journal of Civil Engineering*, vol. 23, no. 2, pp. 923–934, 2019.
- [17] A. Mohanta, K. Patra, and B. Sahoo, "Anticipate Manning's coefficient in meandering compound channels," *Hydrology*, vol. 5, no. 3, p. 47, 2018.
- [18] B. B. Sahoo, R. Jha, A. Singh, and D. Kumar, "Long short-term memory (LSTM) recurrent neural network for low-flow hydrological time series forecasting," *Acta Geophysica*, vol. 67, no. 5, pp. 1471–1481, 2019.
- [19] J. L. Salmeron, M. B. Correia, and P. R. Palos-Sanchez, "Complexity in forecasting and predictive models," *Complexity*, vol. 2019, Article ID 8160659, 3 pages, 2019.
- [20] G.-B. Huang, Q.-Y. Zhu, and C.-K. Siew, "Extreme learning machine: theory and applications," *Neurocomputing*, vol. 70, no. 1–3, pp. 489–501, 2006.
- [21] H. Siqueira, L. Boccato, R. Attux, and C. Lyra, "Unorganized machines for seasonal streamflow series forecasting," *International Journal of Neural Systems*, vol. 24, no. 3, Article ID 1430009, 2014.
- [22] A. R. Lima, A. J. Cannon, and W. W. Hsieh, "Forecasting daily streamflow using online sequential extreme learning machines," *Journal of Hydrology*, vol. 537, pp. 431–443, 2016.
- [23] B. Yadav, S. Ch, S. Mathur, and J. Adamowski, "Discharge forecasting using an online sequential extreme learning machine (OS-ELM) model: a case study in Neckar River, Germany," *Measurement*, vol. 92, pp. 433–445, 2016.
- [24] M. Rezaie-Balf and O. Kisi, "New formulation for forecasting streamflow: evolutionary polynomial regression vs. extreme learning machine," *Hydrology Research*, vol. 49, no. 3, pp. 939–953, 2017.
- [25] Z. M. Yaseen, M. F. Allawi, A. A. Yousif, O. Jaafar, F. M. Hamzah, and A. El-Shafie, "Non-tuned machine learning approach for hydrological time series forecasting," *Neural Computing and Applications*, vol. 30, no. 5, pp. 1479–1491, 2018.
- [26] A. R. Lima, A. J. Cannon, and W. W. Hsieh, "Nonlinear regression in environmental sciences using extreme learning machines: a comparative evaluation," *Environmental Modelling & Software*, vol. 73, pp. 175–188, 2015.
- [27] S. Heddami and O. Kisi, "Extreme learning machines: a new approach for modeling dissolved oxygen (DO) concentration with and without water quality variables as predictors," *Environmental Science and Pollution Research*, vol. 24, no. 20, pp. 16702–16724, 2017.
- [28] S. Heddami, "Use of optimally pruned extreme learning machine (OP-ELM) in forecasting dissolved oxygen concentration (DO) several hours in advance: a case study from the Lamath River, Oregon, USA," *Environmental Processes*, vol. 3, no. 4, pp. 909–937, 2016.
- [29] Z. M. Yaseen, S. M. Awadh, A. Sharafati, and S. Shahid, "Complementary data-intelligence model for river flow simulation," *Journal of Hydrology*, vol. 567, pp. 180–190, 2018.
- [30] P. Mohapatra, K. Nath Das, and S. Roy, "A modified competitive swarm optimizer for large scale optimization problems," *Applied Soft Computing*, vol. 59, pp. 340–362, 2017.
- [31] M. T. Hagan and M. B. Menhaj, "Training feedforward networks with the Marquardt algorithm," *IEEE Transactions on Neural Networks*, vol. 5, no. 6, pp. 989–993, 1994.
- [32] S. Mirjalili, A. H. Gandomi, S. Z. Mirjalili, S. Saremi, H. Faris, and S. M. Mirjalili, "Salp swarm algorithm: a bio-inspired optimizer for engineering design problems," *Advances in Engineering Software*, vol. 114, pp. 163–191, 2017.
- [33] Z. M. Yaseen, O. Jaafar, R. C. Deo et al., "Stream-flow forecasting using extreme learning machines: a case study in a semi-arid region in Iraq," *Journal of Hydrology*, vol. 542, pp. 603–614, 2016.
- [34] G. Huang, G.-B. Huang, S. Song, and K. You, "Trends in extreme learning machines: a review," *Neural Networks*, vol. 61, pp. 32–48, 2015.
- [35] H. Sanikhani, R. C. Deo, Z. M. Yaseen, O. Eray, and O. Kisi, "Non-tuned data intelligent model for soil temperature estimation: a new approach," *Geoderma*, vol. 330, pp. 52–64, 2018.
- [36] M. Eshtay, H. Faris, and N. Obeid, "Improving extreme learning machine by competitive swarm optimization and its

- application for medical diagnosis problems,” *Expert Systems with Applications*, vol. 104, pp. 134–152, 2018.
- [37] N. Al-ansari, M. Abdellatif, M. Ezeelden, S. S. Ali, and S. Knutsson, “Climate change and future long-term trends of rainfall at north-east of Iraq,” *Journal of Civil Engineering and Architecture*, vol. 8, no. 6, pp. 790–805, 2014.
- [38] D. Bozkurt, O. Sen, and S. Hagemann, “Projected river discharge in the Euphrates-Tigris basin from a hydrological discharge model forced with RCM and GCM outputs,” *Climate Research*, vol. 62, no. 2, pp. 131–147, 2015.
- [39] N. Al-Ansari, A. A. Ali, and S. Knutsson, “Present conditions and future challenges of water resources problems in Iraq,” *Journal of Water Resource and Protection*, vol. 6, no. 12, pp. 1066–1098, 2014.
- [40] S. A. Salman, S. Shahid, T. Ismail, N. B. A. Rahman, X. Wang, and E.-S. Chung, “Unidirectional trends in daily rainfall extremes of Iraq,” *Theoretical and Applied Climatology*, vol. 134, no. 3-4, pp. 1165–1177, 2018.
- [41] D. K. Saleh, *Stream Gage Descriptions and Streamflow Statistics for Sites in the Tigris River and Euphrates River Basins, Iraq*, US Department of the Interior, US Geological Survey, Reston, VA, USA, 2010.
- [42] K. P. Sudheer, A. K. Gosain, D. Mohana Rangan, and S. M. Saheb, “Modelling evaporation using an artificial neural network algorithm,” *Hydrological Processes*, vol. 16, no. 16, pp. 3189–3202, 2002.
- [43] Ö. Kisi, “Multi-layer perceptrons with Levenberg-Marquardt training algorithm for suspended sediment concentration prediction and estimation,” *Hydrological Sciences Journal*, vol. 49, pp. 1025–1040, 2004.
- [44] A. A. H. Alwanas, A. A. Al-Musawi, S. Q. Salih, H. Tao, M. Ali, and Z. M. Yaseen, “Load-carrying capacity and mode failure simulation of beam-column joint connection: application of self-tuning machine learning model,” *Engineering Structures*, vol. 194, pp. 220–229, 2019.
- [45] M. Hall, E. Frank, G. Holmes, B. Pfahringer, P. Reutemann, and I. H. Witten, “The WEKA data mining software,” *ACM SIGKDD Explorations Newsletter*, vol. 11, no. 1, p. 10, 2009.
- [46] H. Azimi, H. Bonakdari, I. Ebtehaj, and D. G. Michelson, “A combined adaptive neuro-fuzzy inference system-firefly algorithm model for predicting the roller length of a hydraulic jump on a rough channel bed,” *Neural Computing and Applications*, vol. 29, no. 6, pp. 249–258, 2016.
- [47] M. A. Ghorbani, R. C. Deo, V. Karimi, Z. M. Yaseen, and O. Terzi, “Implementation of a hybrid MLP-FFA model for water level prediction of Lake Egirdir, Turkey,” *Stochastic Environmental Research and Risk Assessment*, vol. 32, no. 6, pp. 1683–1697, 2017.
- [48] Z. M. Yaseen, I. Ebtehaj, H. Bonakdari et al., “Novel approach for streamflow forecasting using a hybrid ANFIS-FFA model,” *Journal of Hydrology*, vol. 554, pp. 263–276, 2017.
- [49] J. Li, H. Ali, A. Samer, S. Hasan et al., “Hybrid soft computing approach for determining water quality indicator: Euphrates River,” *Neural Computing and Applications*, vol. 31, no. 3, pp. 827–837, 2017.
- [50] L. Diop, A. Bodian, K. Djaman et al., “The influence of climatic inputs on stream-flow pattern forecasting: case study of Upper Senegal River,” *Environmental Earth Sciences*, vol. 77, no. 5, p. 182, 2018.
- [51] S. Q. Salih and A. A. Alsewari, “Solving large-scale problems using multi-swarm particle swarm approach,” *International Journal of Engineering & Technology*, vol. 7, no. 3, pp. 1725–1729, 2018.
- [52] S. Q. Salih and A. A. Alsewari, “A new algorithm for normal and large-scale optimization problems: nomadic people optimizer,” *Neural Computing and Applications*, pp. 1–28, 2019, In press.
- [53] H. A. Abdulwahab, A. Noraziah, A. A. Alsewari, and S. Q. Salih, “An enhanced version of black hole algorithm via levy flight for optimization and data clustering problems,” *IEEE Access*, vol. 7, pp. 142085–142096, 2019.